Coordination Chemistry Reviews, 97 (1990) 141–154
Elsevier Science Publishers B.V., Amsterdam — Printed in The Netherlands

ORGANOMETALLIC PHOTOCHEMISTRY : AB INITIO POTENTIAL ENERGY SURFACES AS REACTION MAPS OF THE PRIMARY PHOTOPROCESS

C. DANIEL

ER 139 du CNRS, Laboratoire de Chimie Quantique,
4, rue Blaise Pascal 67000 Strasbourg, FRANCE

ABSTRACT

The mechanism of the primary photoprocess for several photochemical reactions of organometallic molecules will be discussed on the basis of ab initio potential energy curves obtained from Contracted Configuration Interaction calculations based on Complete Active Space SCF wavefunctions.
The photoactive excited states responsible for the photoelimination of molecular hydrogen in $H_2Fe(CO)_4$, the loss of a carbonyl ligand and the homolysis of the metal-hydrogen bond in $HMn(CO)_5$ will be specified as well as the corresponding reaction paths.
The mechanism of the double photochemistry of $HMn(CO)_5$ will be compared to the photoreactivity of $HCo(CO)_4$.

I. INTRODUCTION

Photochemical reactivity of organometallics represents actually one of the most exciting challenges to theoretical chemists. Because of their intrinsically more complicated nature, photochemical reactions in general are very difficult to analyze experimentally to the degree of mechanistic detail to which one has become accustomed in the case of thermal reactions. In spite of the great experimental activity concerning the photochemistry of organometallic molecules, and although sophisticated equipment is now routinely used for detecting intermediates generated by flash photolysis, there are technical limitations when applied to organometallic systems (ref. 1). These limitations are at the origin of the lack of detailed mechanistic informations responsible for many unknowns regarding the events occuring between the initial excitation of the reactant and the formation of the primary product in its ground state.

0010-8545/90/$04.90

Even if a quantitative theoretical study of the dynamics of the reaction is still beyond reach, one may hope that a qualitative approach will serve as a useful systematizing, unifying framework in the consideration of the photoreactivity of organometallic molecules.

Until recently the use of state correlation diagrams which point to the possible pathways interconverting the reactants to the products was the only realistic theoretical method useful to predict the mechanism of the primary photochemical process (refs. 2-5). A particularly powerful means of understanding photochemical processes is possible by considering the potential energy surfaces (PES) or the more readily visualized potential energy curves (PEC) which connect the reactants to the primary products (ref. 6). It is only in the last few years that this approach based on the PES has been applied with success to the photochemistry of organometallic molecules (refs. 7-10).
The calculation of potential energy curves has enabled us to get a better understanding of the mechanism of the photodissociation of a carbonyl ligand from $Fe(CO)_5$ (ref. 7) and $HCo(CO)_4$ (ref. 10) and to understand the existence of two competitive photochemical processes upon irradiation of $HCo(CO)_4$ at a unique wavelength (refs. 8-10).
The present contribution will describe the results which we have obtained for the photoelimination of molecular hydrogen from $H_2Fe(CO)_4$:

$$H_2Fe(CO)_4 \xrightarrow{h\nu} H_2 + Fe(CO)_4$$

The mechanism of the photochemistry of $HMn(CO)_5$ and the occurence of two reactive channels upon irradiation of this molecule at different wavelengths will be discussed :

$$HMn(CO)_5 \xrightarrow{h\nu} H + Mn(CO)_5$$

$$HMn(CO)_5 \xrightarrow{h\nu} HMn(CO)_4 + CO$$

Finally the photoreactivity of this complex will be compared to that of $HCo(CO)_4$.

II. THE METHOD OF CALCULATION

A detailed description of the method used to reproduce correctly the sequence and energetics of electronic states of the reactant and products is described elsewhere (ref. 9). Ab initio potential energy curves are obtained from Contracted Configuration Interaction calculations based on a CASSCF (Complete Active Space SCF) reference wavefunction. Details of the CASSCF calculations are reported in Table 1. in which the active space is discribed by the number of electrons correleted (ne) and the number of active orbitals (na).

TABLE 1

The CASSCF calculations.

	State	MainConfiguration[a]	Active Space
$H_2Fe(CO)_4$	$^5A_1$	$(\sigma_g)^2(3d_{y2-z2})^1(\sigma_g^*)^1(\sigma_u)^1(\sigma_u^*)^1$	6e 6a
$HMn(CO)_5$	$^5A_2$	$(3d_{xy})^2(3d_\pi)^2(\sigma)^2(\sigma^*)^1(3d_{x2-y2})^1$	8e 9a

[a] σ_g and σ_g^* denote the bonding combinations of the two hydrogen s orbitals which are respectively bonding and antibonding with respect to the Fe-H bonds. σ_u and σ_u^* are the antibonding combinations of the two hydrogen s orbitals which are respectively bonding and antibonding with respect to the Fe-H bonds. σ and σ^* denote the MO'S which are respectively bonding and antibonding with respect to the Mn-H bond.

For each electronic state, two CCI calculations were performed : the first one with one reference configuration corresponding to the required state, the second one being a multireference calculation including all the configurations

which appear with a coefficient larger than 0.08 in the moreference CI wavefunction. Details of the CCI calculations are given in Table 2. Ten electrons (in $H_2Fe(CO)_4$) and eight electrons (in $HMn(CO)_5$) are correlated in these calculations (the 3d electrons and those of the M-H bonds). Single and double excitations to all virtual orbitals, except the counterparts of the carbonyl 1s and of the metal 1s 2s and 2p orbitals, are included in the CCI calculations.

TABLE 2

The CCI calculations.

	Valence Space	Nb. of electrons correlated	Nb. of Reference States[a]	Nb. of Config.[a]
$H_2Fe(CO)_4$	$3d_{y2-z2}$, $3d_{xz}$, $3d_{xy}$, σ_g, σ_u, σ_g^*, σ_u^*	10	3 to 6	38736 to 404208
$HMn(CO)_5$	$3d_{xy}$, $3d_{\pi}$, $3d_{x2-y2}$, σ, σ^*	8	2 to 5	26193 to 298125

[a] The number of reference states and of configurations depend on the characteristics of the calculated state (symmetry, spin).

The calculations for $H_2Fe(CO)_4$ and $HMn(CO)_5$ were performed for the experimental geometries (ref. 11) which are of C_{2v} and C_{4v} symmetry respectively.

SCHEME I

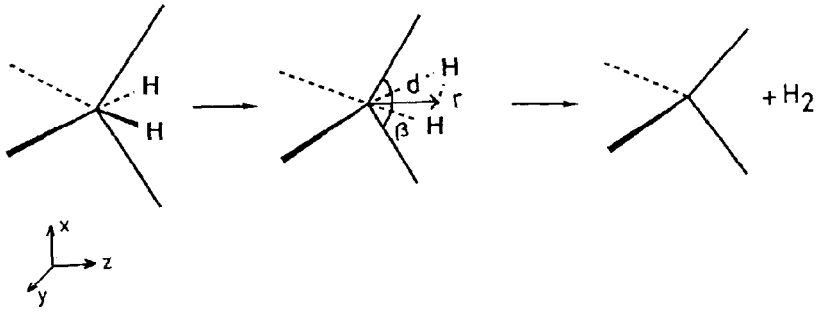

For the photoelimination of molecular hydrogen from $H_2Fe(CO)_4$ it was assumed that the C_{2v} symmetry is retained along the reaction path (Scheme I), since $Fe(CO)_4$ has the C_{2v} symmetry in its ground state (Refs. 7-12). The geometrical parameters d, r and β were optimized for each point along the reaction path at the SCF level for the ground state of the reactant (ref. 13).
Similarly, it has been assumed that the C_{4v} symmetry is retained along the reaction path corresponding to the homolysis of the metal hydrogen bond (Scheme II), since $Mn(CO)_5$ has the C_{4v} symmetry in its ground state (refs. 14-15).

SCHEME II

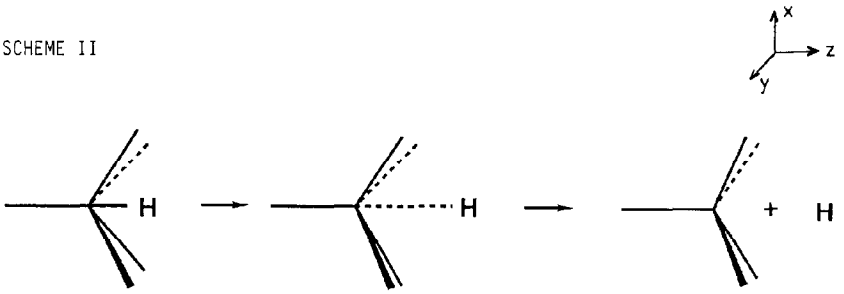

For the photodissociation of a carbonyl ligand from $HMn(CO)_5$ we have considered only the loss of an axial ligand which produces $HMn(CO)_4$ as a square pyramid of C_{4v} symmetry with the hydrogen atom in apical position. For this reason we have assumed that the C_{4v} symmetry is retained along the reaction path (Scheme III).

SCHEME III

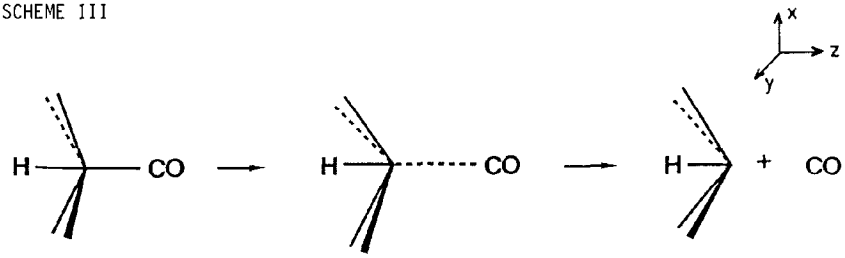

The following gaussian basis sets were used : for the transition metal a (15,11,6) set contracted to (9,6,3) (ref. 16), for the first row atoms a (10,6) set contracted to (4,2) (ref. 17) and for hydrogen a (6,1) set contracted to (3,1) (ref. 18). This basis set is triple-zeta for the 1s shell of hydrogen and for the 3d and 4s shells of the transition atoms, and otherwise it is double-zeta.

III. THE PHOTOELIMINATION OF MOLECULAR HYDROGEN FROM $H_2Fe(CO)_4$.

When $H_2Fe(CO)_4$ is irradiated in a low temperature matrix the primary process is the loss of dihydrogen (followed with an oxidative addition) (ref. 19) :

$$H_2Fe(CO)_4 \underset{\text{visible light}}{\overset{\text{uv photolysis}}{\rightleftharpoons}} H_2 + Fe(CO)_4$$

The potential energy curves of Fig. 1 for the states $^1A_1$ (ground state) and $^{1,3}B_2$ form the basis for a qualitative understanding of the mechanism of the photoelimination of molecular hydrogen (ref. 20) :

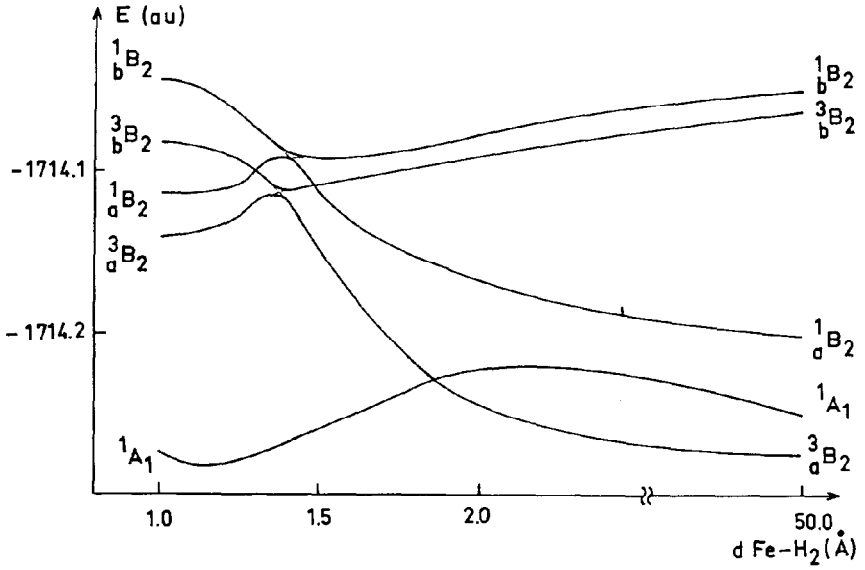

Fig. 1. CCI potential energy curves for the elimination of H_2 in $H_2Fe(CO)_4$.

Excitation at 254nm (39370 cm^{-1}) will bring the molecule from the ground state $^1A_1$ to the lowest $^1B_2$ excited state (denoted $^1_aB_2$ and calculated at 35189 cm^{-1}). From there the system has the possibilities to evolve to the products H_2 and $Fe(CO)_4$ in their ground states by two different mechanisms :

i) intersystem crossing to the highest $^3B_2$ excited state (denoted $^3_bB_2$) around 1.30 A followed with internal conversion to the lowest $^3B_2$ excited state (denoted $^3_aB_2$). From there photoelimination of molecular hydrogen takes place along the $^3_aB_2$ potential energy curve with the system going downhill to the products.

ii) or intersystem crossing to the lowest $^3_aB_2$ excited state with photoelimination of hydrogen occuring along the $^3_aB_2$ potential energy curve with a small energy barrier (of the order of 10 kcal/mole).

The reverse reaction, namely the oxidative addition of molecular hydrogen to $Fe(CO)_4$ should be both spin and symmetry forbidden since the ground state is $^3B_2$ for $Fe(CO)_4$ and $^1A_1$ for $H_2Fe(CO)_4$. However, this reaction is presumed to take place under visible irradiation at low temperature (ref. 19). It is possible to reconcile the possibility of a reverse reaction with the spin and symmetry conservation rules by introducing spin-orbit coupling.

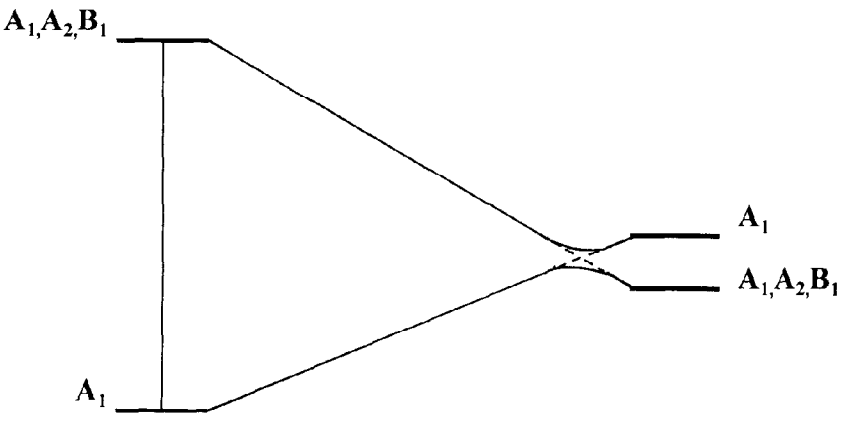

Fig. 2. State correlation diagram for the elimination of H_2 from $H_2Fe(CO)_4$ with spin orbit coupling.

As the reaction of H_2 and $Fe(CO)_4$ is analogous to the recombination of $Fe(CO)_4$ with CO (ref. 21) which should also be forbidden, we shall use the same explanation based on spin-orbit coupling consideration (ref. 4) : the spin-orbit coupling operator does split the $^3B_2$ ground state of the products in three states A_1, A_2, and B_1.
This results in avoidance of the A_1 curves, with a potential energy curve of symmetry A_1 connecting the ground states of the reactants and products (Fig. 2).

The reverse reaction as well as the direct thermal process becomes now symmetry allowed with a low energy barrier for the reverse reaction. The probability of these two reactions will depend on the efficiency of the spin-orbit coupling.

IV. THE PHOTOCHEMISTRY OF $HMn(CO)_5$.

Although $HMn(CO)_5$ was one of the first transition metal carbonyls to be studied in rare-gas matrices (ref. 22), the mechanism of its photochemistry is only partially understood. Upon irradiation in low temperature matrices $HMn(CO)_5$ undergoes two different photochemical reactions :

i) the heterolytic loss of a carbonyl ligand upon irradiation at 229 nm,

$$HMn(CO)_5 \xrightarrow{h\nu} HMn(CO)_4 + CO$$

ii) the homolysis of the metal-hydrogen bond after prolonged irradiation at 193 nm,

$$HMn(CO)_5 \xrightarrow{h\nu} H + Mn(CO)_5$$

Fig. 3 shows a qualitative set of potential energy surfaces for the ground and excited states of $HMn(CO)_5$ inferred from the potential energy curves calculated for the loss of either the hydrogen or the axial carbonyl ligand (ref. 20). These surfaces form the basis for a qualitative understanding of the mechanism of the photochemistry of $HMn(CO)_5$:

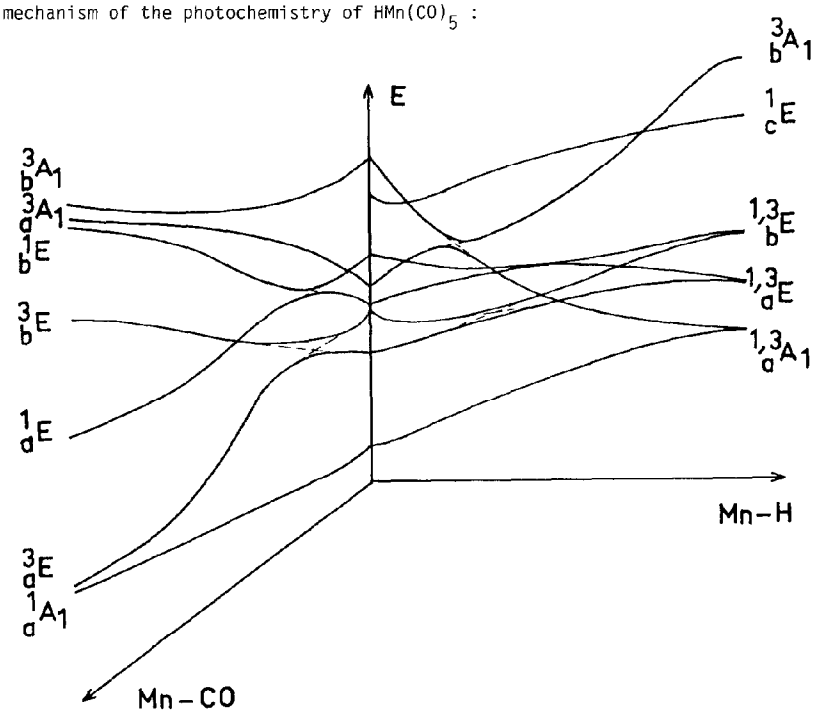

Fig. 3. Potential energy surfaces corresponding to the loss of hydrogen and axial carbonyl ligand in $HMn(CO)_5$.

Irradiation at 229nm (43668 cm^{-1}) will bring the molecule in the ^1E_b state (calculated at 43152 cm^{-1}). From there, the molecule goes down along the ^1E_b curve corresponding to Mn-CO elongation until it reaches a potential well corresponding to an avoided crossing. At this point, the system evolves to the ^1E_a state through internal conversion and dissociation to the products CO and $HMn(CO)_4$ will then occur along the ^1E_a curve. However this mechanism produces $HMn(CO)_4$ as a square pyramid with H apical, with a subsequent Berry pseudorotation yielding the square pyramid with H basal (Scheme IV) (ref. 5-23), corresponding to the isomer which has been identified experimentally (ref. 22).

SCHEME IV

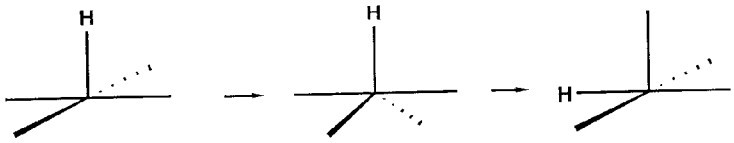

Excitation at a lower energy (λ > 285 nm, or < 35000 cm^{-1}) will bring the molecule from the $^1A_1$ ground state into the ^1_aE excited state (calculated at 33579 cm^{-1}). After intersystem crossing to the state ^3_bE (calculated separation less than 1000 cm^{-1}) the molecule gets trapped into the ^3_bE potential energy curve corresponding to Mn-CO elongation. Through internal conversion to the lowest ^3_aE state the system will dissociate along the corresponding ^3_aE potential energy curve to the products CO and $HMn(CO)_4$, the latter as a square pyramid with H apical in the ^3_aE state. The close proximity of the ^3_aE and $^1A_1$ states at dissociation (calculated separation less than 2000 cm^{-1}) makes the intersystem crossing between them an easy process. Then the reverse addition reaction can take place without any barrier along the $^1A_1$ potential energy curve to regenerate $HMn(CO)_5$ in its ground state accordingly to the experimental findings (ref. 24).

Excitation at 193 nm (51813 cm^{-1}) will bring the molecule from the state $^1A_1$ into the highest ^1_cE excited state (calculated at 53900 cm^{-1}). Intersystem crossing (around d_{M-H} = 1.2 A) will bring the system first into the potential energy curve $^3_bA_1$ and next through internal conversion into the $^3_aA_1$ $\sigma \longrightarrow \sigma^*$ potential energy curve. From there the molecule will dissociate along this $^3_aA_1$ potential energy curve to the products H and $Mn(CO)_5$ in their ground state $^{1,3}A_1$.

It seems rather clear from a look at the surfaces of Fig. 3 that a high excitation energy will be necessary to cleave the metal hydrogen bond in $HMn(CO)_5$, since the lowest excited states $^{1,3}E$ are dissociative with respect to the carbonyl loss but correspond to repulsive potential energy curves with respect to the dissociation of the metal-hydrogen bond. In order to find potential energy curves which are dissociative with respect to the metal-hydrogen bond in the vicinity of the equilibrium distance, one has to consider either the $^3_bA_1$ or the ^1_cE states, both being at relatively high energy (> 50000 cm^{-1}).

V. DISSIMILARITY BETWEEN THE PHOTOREACTIVITIES OF $HMn(CO)_5$ AND $HCo(CO)_4$.

Since metal-hydrogen and metal-carbonyl bond energies are very similar for the two systems (ref. 25-26), it is surprising that the homolysis of the metal hydrogen bond and the carbonyl loss do occur at the same wavelength for $HCo(CO)_4$ but at different wavelengthes for $HMn(CO)_5$. It could be fruitful to compare the most important features of their photochemistry (ref. 10-20) and to understand the reasons of their dissimilarities.

The principal reason for this different behavior seems to be the high density of states in the lowest part of the electronic spectrum in $HMn(CO)_5$ (ref. 20) which is a consequence of the electronic configuration of this system. The presence of two vacant orbitals $3d_{x2-y2}$ and σ^* is responsible for the great number of low excited states susceptible to play a key role in the photochemistry of $HMn(CO)_5$ compared to the situation for $HCo(CO)_4$ with only one empty orbital σ^*. Indeed if the potential energy surfaces corresponding to the two concurrent processes are relatively simple in the case of $HCo(CO)_4$ (ref. 10), they look much more complex (presence of avoided crossing and energy barriers) in the case of $HMn(CO)_5$.

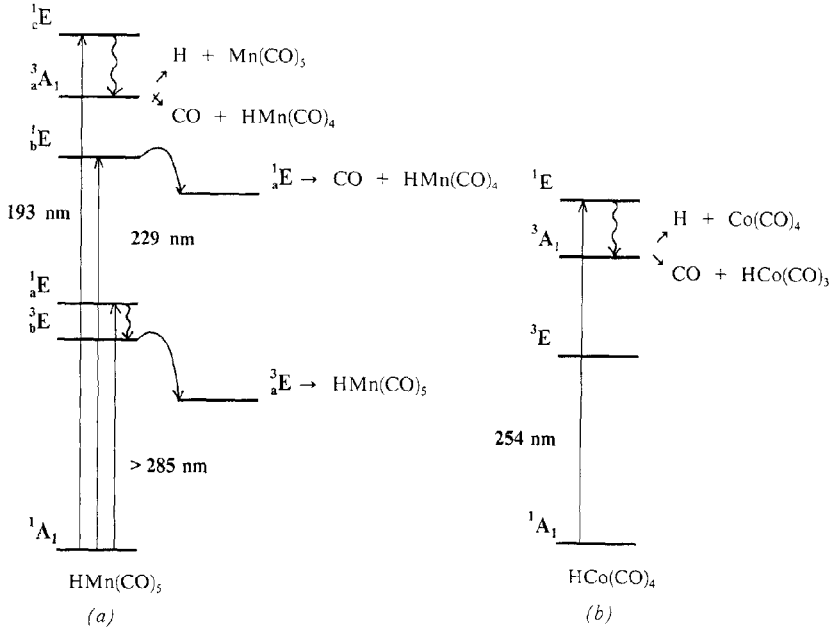

Fig. 4. State diagrams for the photochemistry of $HMn(CO)_5$ (this work) and $HCo(CO)_4$ (ref. 10).

The state diagrams, not to be confounded with the state correlation diagrams, depicting the photochemistry of $HMn(CO)_5$ (Fig. 4(a)) and $HCo(CO)_4$ (Fig. 4(b)) outline the main differences concerning the photoreactivity of the two molecules.

The presence of a low lying ^1_aE LF state in $HMn(CO)_5$ raises the energy of the ^1_bE state and this is responsible for the relative high energy (calculated at 43152 cm^{-1} in $HMn(CO)_5$ to be compared to 36000 cm^{-1} in $HCo(CO)_4$) of the photoactive ^1E $d \longrightarrow \sigma^*$ excited state for the dissociation of the carbonyl ligand. Moreover this low LF ^1_aE state in $HMn(CO)_5$ is desactivated with respect to the carbonyl loss because of its close proximity to the ^3_bE $d \longrightarrow \sigma^*$ state which is the precursor of the reverse reaction. In $HCo(CO)_4$ the excited state $^3A_1$ $\sigma \longrightarrow \sigma^*$ is dissociative for both the hydrogen and the carbonyl loss. The situation is quite different in $HMn(CO)_5$ where only the states $^{1,3}E$ $d \longrightarrow \sigma^*$ are dissociative for the decarbonylation.

VI. CONCLUSION

From the results reported above it seems clear that theoretical studies can contribute to the elucidation of the mechanism of the photochemical reactions of organometallics.

Mapping of pontential energy surfaces provides a better understanding of concurrent photochemical reactions (occurence of two reactive channels upon irradiation either at a unique wavelength or at different wavelengthes). To make further progress, analysis of the dynamics of the processes occuring on these surfaces is needed.

A quantitative theoretical study leading to an evaluation of spin - orbit coupling as well as to an estimate of the lifetime of the excited states should enable us to get informations concerning the efficiency of the expected photoprocesses.

Acknowledgements

The calculations have been carried out on the CRAY-2 computer of the CCVR (Palaiseau, France) through a grant of computer time from the Conseil Scientifique du Centre de Calcul Vectoriel pour la Recherche.

REFERENCES

1 M. Poliakoff, E. Weitz, Advances in Organometallic Chemistry, vol.25 (1986) 277-316.

2 A. Veillard, Nouv. J. Chim., 5 (1981) 599-601.

3 A. Veillard, A. Dedieu, Nouv. J. Chim., 7 (1983) 683-686.

4 A. Veillard, A. Dedieu, Theoret. Chim. Act., 63 (1983) 339-348.

5 C. Daniel, A. Veillard, Nouv. J. Chim., 10 (1986) 83-90.

6 N. J. Turro, Modern molecular photochemistry, The Benjamin/ Cummings Publishing Company, Inc., Menlo Park Ca., 1978.

7 C. Daniel, M. Benard, A. Dedieu, R. Wiest, A. Veillard, J. Phys. Chem., 21 (1984) 4805-4811.

8 C. Daniel, I. Hyla-Kryspin, J. Demuynck, A. Veillard, Nouv. J. Chim., 9 (1985) 581-590.

9 A. Veillard, C. Daniel, A. Strich, Pure & Appl. Chem., 60(2) (1988) 215-221.

10 A. Veillard, A. Strich, J. Am. Chem. Soc., 110 (1988) 3793-3797.

11 E.A. McNeill and F.R. Scholer, J. Am. Chem. Soc., 99 (1977) 6243-6249.

12 M. Poliakoff, J.J. Turner, J. Chem. Soc. Dalton Trans., (1974) 2276-2285.

13 I. Hyla-Kryspin, A. Dedieu, unpublished.

14 S.P. Church, M. Poliakoff, J. A. Timney and J.J. Turner, J. Am. Chem. Soc., 103 (1981) 7515-7520.

15 C. Daniel, unpublished.

16 A. J. H. Wachters, J. Chem. Phys., 52 (1970) 1033-1036.

17 S. Huzinaga, Approximate atomic functions, Technical Report, University of Alberta, Alberta (1971).

18 S. Huzinaga, J. Chem. Phys., 42 (1965) 1293-1302.

19 R. L. Sweany, J. Am. Chem. Soc., 103 (1981) 2410-2412.

20 C. Daniel, in preparation.

21 B. Davies, A. Mc Neish, M. Poliakoff, J.J. Turner, J. Am. Chem. Soc., 99 (1977) 7573-7579.

22 S.P. Church, M. Poliakoff, J. A. Timney, J. J. Turner, Inorg. Chem., 22 (1983) 3259-3266.

23 Preliminary SCF calculations indicate that $HMn(CO)_4$ with H in basal position is more stable than the square pyramid with H in apical position by around 15 kcal/mole.

24. A. J. Rest, J. J. Turner, J. Chem. Soc., Chem. Comm., 375-377 (1969).

25 T. Ziegler, V. Tschinke, A. Becke, J. Am. Chem. Soc., 109 (1987) 1351-1358.

26 T. Ziegler, V. Tschinke, C. Ursenbach, J. Am. Chem. Soc., 109 (1987) 4825-4837.